Entanglement-enabled delayed choice experiment

Florian Kaiser, Thomas Coudreau, Perola Milman, Daniel Barry Ostrowsky, Sébastien Tanzilli

Entanglement-enabled delayed choice experiment

Florian Kaiser,[1] Thomas Coudreau,[2] Perola Milman,[2,3]
Daniel B. Ostrowsky,[1] Sébastien Tanzilli[1*]

[1] Laboratoire de Physique de la Matière Condensée, CNRS UMR 7336,
Université de Nice – Sophia Antipolis, Parc Valrose, 06108 Nice Cedex 2, France

[2] Université Paris Diderot, Sorbonne Paris Cité,
Laboratoire Matériaux et Phénomènes Quantiques, CNRS, UMR 7162, 75013 Paris, France

[3] Université Paris Sud 11, Institut de Sciences Moléculaires d'Orsay (CNRS)
Bât. 210, Campus d'Orsay, 91405, Orsay Cedex, France

[*]To whom correspondence should be addressed; E-mail: sebastien.tanzilli@unice.fr

Wave-particle complementarity is one of the most intriguing features of quantum physics. To emphasize this measurement apparatus dependent nature, experiments have been performed in which the output beam-splitter of a Mach-Zehnder interferometer is inserted or removed after a photon has already entered the device. A recent extension suggested using a 'quantum beam-splitter' at the interferometer's output. We realize this using pairs of polarization entangled photons. One photon is tested in the interferometer and is detected, while the other allows determining whether wave, particle, or intermediate behavior have been observed. Furthermore, this allows continuously morphing the tested photon's behavior from wave like to particle like. This illustrates the inadequacy of a naive wave or particle description of light.

While the predictions of quantum mechanics have been verified with remarkable precision, subtle questions arise when attempting to describe quantum phenomena in classical terms (*1,2*). For example, a single quantum object can behave as a wave or as a particle, which is illustrated by Bohr's complementarity principle (*3*). It states that, depending on the measurement apparatus, either wave or particle behavior is observed (*4,5*). This is demonstrated by sending single photons into a Mach-Zehnder interferometer (MZI) followed by two detectors (*6*) (Fig. 1A). If the MZI is closed, *i.e.* the paths of the interferometer are recombined at the output beam-splitter (BS_2), the probabilities for a photon to exit at detectors D_a and D_b depend on the phase difference θ between the two arms. The which-path information remains unknown, and wave-like intensity interference patterns are observed (Fig. 1B). On the other hand, if the MZI is open, *i.e.* BS_2 is removed, each photon's path can be known and, consequently, no interference occurs. Particle behavior is said to be observed and the detection probabilities at D_a and D_b are equal to $\frac{1}{2}$, independently of the value of θ (Fig. 1C). In other words, these two different configurations, *i.e.* BS_2 present or absent, give different experimental results. Recently it has been shown that, even when performing Wheeler's original gedanken experiment (*7*), in which the configuration for BS_2 is chosen only after the photon has passed the entrance beam-splitter BS_1, Bohr's complementarity principle is still obeyed (*8*). Intermediate cases, in which BS_2 is only partially present, have been considered in theory and led to a more general description of Bohr's complementarity principle expressed by an inequality limiting the simultaneously available amount of interference (signature of wave-like behavior) and which path information (particle-like behavior) (*9, 10*). This inequality has also been confirmed experimentally in delayed choice configurations (*11, 12*).

We take Wheeler's experiment one step further by replacing the output beam-splitter by a quantum beam-splitter (QBS), as recently proposed theoretically (*13, 14*). In our realization (Fig. 2), we exploit polarization entanglement as a resource for two reasons. First, doing so per-

mits implementing the QBS. Second, it allows us to use one of the entangled photons as a test photon sent to the interferometer, and the other one as a corroborative photon. Here, as opposed to previous experiments (*8, 11*), the state of the interferometer remains unknown, and therefore the wave or particle behavior of the test photon, until we detect the corroborative photon. By continuously modifying the type of measurement performed on the corroborative photon, we can morph the test photon from wave to particle behavior, even after the test photon was detected. To exclude interpretations based on either mixed states, associated with pre-existing state information (*15*), or potential communication between the two photons, the presence of entanglement is verified via violation of the Bell inequalities with a space-like separation (*16–18*).

The QBS is based on the idea that when a photon in an arbitrary polarization state enters an interferometer that is open for $|H\rangle$ (horizontally polarized) and closed for $|V\rangle$ (vertically polarized) photons, the states of the interferometer and the photon become correlated. Our apparatus, shown in the right hand side of Fig. 2 and detailed in Fig. S1, therefore reveals a particle behavior for the $|H\rangle$ component of the photon state, and a wave behavior for the $|V\rangle$ component. Note that such an experiment has been realized using single photons prepared in a coherent superposition of $|H\rangle$ and $|V\rangle$ (*12*). However, we take this idea a step further by achieving genuine quantum behavior for the output beam-splitter by exploiting an intrinsically quantum resource, entanglement. This allows entangling the quantum beam-splitter and test photon system with the corroborative photon. Thus, measurement of the corroborative photon enables projecting the test photon/QBS system into an arbitrary coherent wave-particle superposition, which is a purely quantum object. In other words, our QBS is measured by another quantum object, which projects it into a particular superposition of present and absent states. More precisely, we use as a test photon one of the photons from the maximally polarization entangled Bell state, $|\Phi^+\rangle = \frac{1}{\sqrt{2}}\left(c_H^\dagger t_H^\dagger + c_V^\dagger t_V^\dagger\right)|vac\rangle$, produced at the wavelength of 1560 nm using the source described in (*19*). Here, using the notation of Fig. 2, $c_H^\dagger$ ($t_H^\dagger$) and $c_V^\dagger$ ($t_V^\dagger$) rep-

resent creation operators for horizontally and vertically polarized photonic modes, respectively, propagating towards the corroborative (test) photon apparatus. Moreover, $|vac\rangle$ represents the vacuum state. Using an entangled state of this form ensures maximum randomness of the input polarization state of the test photon (t), which enters a Mach-Zehnder interferometer with a QBS for the output beam-splitter.

The actual QBS device is made up of two components. The first is a polarization dependent beam-splitter (PDBS) that shows close to 100% reflection for horizontally polarized photons and provides ordinary 50/50 splitting ratio for the vertically polarized photons. The PDBS is realized using a combination of standard bulk optical components as described in supplementary information S1. The whole state after the PDBS reads

$$|\Psi\rangle = \frac{1}{2}\left(c_H^\dagger \left(-e^{i\,\theta}\, a_H^\dagger + i\, b_H^\dagger +\right) + \frac{1}{\sqrt{2}} c_V^\dagger \left(b_V^\dagger (i + i\, e^{i\,\theta}) + a_V^\dagger (1 - e^{i\,\theta})\right)\right)|vac\rangle. \quad (1)$$

Here, θ is an adjustable phase shift in the interferometer, while $a_H^\dagger$, $a_V^\dagger$, $b_H^\dagger$, and $b_V^\dagger$ symbolize creation operators for test photons propagating toward PBS_1 and PBS_2, respectively. At this point, each polarization state of the test photon is associated with one of the two complementary types of behaviors, wave and particle.

The second stage consists of polarizing beam-splitters (PBS_1 and PBS_2) oriented at 45° to the $\{H, V\}$ basis, that permits erasing all polarization information that existed at the PDBS output (*4, 5, 20*). Eq. 1 becomes

$$|\Psi\rangle = \frac{1}{\sqrt{2}}\left(c_H^\dagger [particle]^\dagger + c_V^\dagger [wave]^\dagger\right)|vac\rangle, \quad (2)$$

with

$$[particle]^\dagger = \frac{1}{2}\left(-e^{i\,\theta}(a'^\dagger + a''^\dagger) + i(b'^\dagger + b''^\dagger)\right),$$

and

$$[wave]^\dagger = \frac{1}{2\sqrt{2}}\left((1 - e^{i\,\theta})(-a'^\dagger + a''^\dagger) + i(1 + e^{i\,\theta})(-b'^\dagger + b''^\dagger)\right).$$

Here, the creation operators $a'^{\dagger}$, $a''^{\dagger}$, $b'^{\dagger}$ and $b''^{\dagger}$ denote photons propagating toward detectors $\mathrm{D}_{a'}$, $\mathrm{D}_{a''}$, $\mathrm{D}_{b'}$ and $\mathrm{D}_{b''}$, respectively. Consequently, the only way of knowing if wave or particle behavior was observed is by examining the corroborative photon.

The corroborative photon measurement apparatus, as shown on the left-hand side of Fig. 2. consists of two stages. The first is an electro-optic phase modulator (EOM) that allows rotating the polarization state of the corroborative photon by an angle α. From Eq. 2, we now have

$$|\Psi\rangle = \frac{1}{\sqrt{2}}\left(c_H^{\dagger}(\cos\alpha[particle]^{\dagger} - \sin\alpha[wave]^{\dagger}) + c_V^{\dagger}(\cos\alpha[wave]^{\dagger} + \sin\alpha[particle]^{\dagger})\right)|vac\rangle. \tag{3}$$

After passing PBS_3, that is oriented on the $\{H, V\}$ axis, the corroborative photon is transmitted ($|H\rangle$) or reflected ($|V\rangle$). This projects the test photon into a state defined by the terms in the parentheses of Eq. 3. Therefore, the firing of detector D_H indicates that the test photon is in the state $\cos\alpha[particle]^{\dagger} - \sin\alpha[wave]^{\dagger}$, while the firing of D_V that it is in the state $\cos\alpha[wave]^{\dagger} + \sin\alpha[particle]^{\dagger}$. It can be seen that by choosing $0 < \alpha < 90°$, a continuous morphing between wave and particle behavior is obtained. The expected intensity correlations, given by the coincidence count probability between detectors D_H (corroborative) and $[\mathrm{D}_{b'} \oplus \mathrm{D}_{b''}]$ (test), where $\oplus$ denotes an exclusive OR (XOR) gate, are

$$I_{H,b}(\theta, \alpha) = \cos^2\frac{\theta}{2}\,\sin^2\alpha + \frac{1}{2}\cos^2\alpha. \tag{4}$$

Note that the correlations between detectors D_V and $[\mathrm{D}_{a'} \oplus \mathrm{D}_{a''}]$ follow the same function. On the contrary the complementary intensity correlations, *i.e.* between detectors D_H and $[\mathrm{D}_{a'} \oplus \mathrm{D}_{a''}]$ or between D_V and $[\mathrm{D}_{b'} \oplus \mathrm{D}_{b''}]$, are given by $1 - I_{H,b}(\theta, \alpha)$. The use of XOR gates permits counting the photons from both outputs of each quantum eraser (PBS_1 or PBS_2), and reaching an average coincidence rate of 70/s for each of them. Note that Eq. 4 does not depend on the relative detection times of the two photons. In the experiment reported here, the detection of the corroborative photon is delayed until after the detection of the test photon. This is ensured

by inserting an extra 5 m length of optical fiber in the path of the corroborative photon (c). In this case, for all the four correlation functions mentioned above, the configuration of the interferometer remains undetermined even after the test photon has been detected. In other words, there is no information available yet from the corroborative photon that could influence the behavior of the test photon. Furthermore, a space-time analysis shows that no classical communication can be established between the photon detection events, as they are space-like separated (Fig. 3).

We now measure the correlations between detectors D_H and $[\mathrm{D}_{b'} \oplus \mathrm{D}_{b''}]$ via counting coincidence events on the corresponding single photon detectors (InGaAs avalanche photodiodes). As shown in Fig. 4(A), the experimentally measured results are in near perfect agreement with the theoretical predictions of Eq. 4. For the angle $\alpha = 0°$, $I_{H,b}(\theta, 0)$ is independent of the phase θ as predicted for particle-like behavior. Setting $\alpha = 90°$ results in sinusoidal intensity oscillations as a function of θ, which corresponds to wave-like behavior. For $0° < \alpha < 90°$, a continuous transition from wave to particle behavior is observed, expressed by the continually reducing fringe visibility. As outlined in references (*9, 10*), a generalization of Bohr's complementarity principle implies the interference fringe visibility V and the path distinguishability D, also called the which-way information, to be limited by the following inequality

$$V^2 + D^2 \leq 1. \tag{5}$$

The experimental measurement of these two quantities is described in supplementary information S2 (*11, 12*). Fig. 4(B) shows the obtained results for V^2, D^2 and $V^2 + D^2$ as a function of the angle α. With our experimental data, Eq. 5 is confirmed for all angles of α.

To prove the existence of a coherent quantum superposition of wave and particle behavior of the test photon created by the detection of the corroborative photon, the presence of entanglement needs to be verified (*16,21*). Note that several recent realizations ignored this and therefore

the presence of a QBS has not been proven unambiguously (*22, 23*). In our realization, entanglement is proven by performing the same experiment as before, but using the complementary analysis basis, namely the diagonal basis $\{D, A\}$. Now, the initial quantum state is rotated by 45°, *i.e.* $\frac{1}{\sqrt{2}}\left(c_V^\dagger t_V^\dagger + c_H^\dagger t_H^\dagger\right)|vac\rangle \rightarrow \frac{1}{\sqrt{2}}\left(c_D^\dagger t_D^\dagger + c_A^\dagger t_A^\dagger\right)|vac\rangle$, where D and A symbolize diagonally and anti-diagonally polarized photon contributions, respectively. In this configuration, every single photon is unpredictably subjected to a closed or open Mach-Zehnder configuration by the PDBS. In this case, as opposed to the experiment in the $\{H, V\}$ basis, if a statistical mixture was analysed instead of an entangled state, no correlations should be observed when measuring $I_{H,b}(\theta, \alpha)$. However, the strong correlations shown in Fig. 4(C) exclude a statistical mixture and are in good agreement with the theoretical predictions of Eq. 4. This underlines that wave and particle behavior coexist simultaneously for the entire range $0° < \alpha < 90°$ in the $\{H,\, V\}$ basis, and for $-45° < \alpha < 45°$ in the $\{D,\, A\}$ basis. Fig. 4(D) shows the measurements for V^2, D^2 and $V^2 + D^2$ as a function of α and confirms the upper limits imposed by Eq. 5. The quality of the entangled state is measured via the Bell parameter S, which is deduced from the phase oscillation visibilities at $\alpha = 90°$ in the $\{H,\, V\}$ basis, and $\alpha = 45°$ in the $\{D,\, A\}$ basis. We obtain $S = 2.77 \pm 0.07$, which is very close to the optimal value of $2\sqrt{2}$ attained with maximally entangled states, and 11 standard deviations above the classical/quantum boundary $S = 2$ (*16, 21*).

We note that the detection loophole remains open in our experiment, since some of the initial entangled photons are lost during their propagation in the fiber or bulk channels, or are not detected by the single photon detectors that show non-unit quantum detection efficiencies (*24*). We therefore make the reasonable assumption that the detected photons represent a faithful sample (*17*).

In conclusion, we have carried out a quantum delayed choice experiment, enabled by polarization entangled photons and the associated property of non-locality. We used a Mach-Zehnder

interferometer where the output beam-splitter has been replaced by its quantum analogue, *i.e.* a beam-splitter in a coherent superposition of being present and absent. In this configuration, we observed that the single photons under test can indeed behave as waves and particles in the same experiment, meaning that the simple view of photons being either waves or particles is refuted. We experimentally excluded interpretations based on local hidden variables and/or information exchange between the photon and the quantum beam-splitter. The state of the quantum beam-splitter is determined by the detection of the corroborative photon. We have, therefore, demonstrated delayed interference between wave and particle behavior, which underlines the subtleness of Bohr's complementarity principle.

We note that, parallel to this work, Peruzzo *et al.* realized another version of a quantum delayed choice experiment based on entangled photons (*25*).

References and Notes

1. E. Schrödinger, *Die gegenwärtige Situation in der Quantenmechanik*, Naturwissenschaften **23**, pp. 807-812 (1935).
2. G. Greenstein, A. Zajonc, *The Quantum Challenge: Modern Research On The Foundations Of Quantum Mechanics* (Jones and Bertlett Publishers, Sudbury, 2006).
3. N. Bohr, *in Quantum Theory and Measurement*, J.A. Wheeler, W.H. Zurek, Eds. (Princeton Univ. Press, Princeton, NJ), p. 949, (1984).
4. Y.-H. Kim, R. Yu, S.P. Kulik, Y. Shih, and M.O. Scully, *Delayed choice quantum eraser*, Phys. Rev. Lett. **84**, pp. 1-5 (2000).
5. S. P. Walborn, M. O. Terra Cunha, S. Pádua, and C. H. Monken, *Double-slit quantum eraser*, Phys. Rev. A **65**, 033818 (2002).
6. P. Grangier, G. Roger, A. Aspect, *Experimental Evidence for a Photon Anticorrelation Effect on a beam-splitter: A New Light on Single-Photon Interferences*, EPL **1**, 173 (1986).
7. J. A. Wheeler, in *Quantum Theory and Measurement*, J. A. Wheeler, W. H. Zurek, Eds. (Princeton Univ. Press, Princeton, NJ, 1984), 182–213.
8. V. Jacques, E Wu, F. Grosshans, F. Treussart, P. Grangier, A. Aspect, J.-F. Roch, *Experimental Realization of Wheeler's Delayed-Choice Gedanken Experiment*, Science **315**, pp. 966-968 (2007).
9. W. K. Wootters, W. H. Zurek, *Complementarity in the double-slit experiment: Quantum nonseparability and a quantitative statement of Bohr's principle*. Phys. Rev. D **19**, pp. 473–484 (1978).
10. B.-G. Englert, *Fringe Visibility and Which-Way Information: An Inequality*. Phys. Rev. Lett. **77**, pp. 2154–2157 (1996).
11. V. Jacques, E. Wu, F. Grosshans, F. Treussart, P. Grangier, *Delayed-Choice Test of Quantum Complementarity with Interfering Single Photons*. Phys. Rev. Lett. **100**, 220402 (2008).
12. J.-S. Tang, Y.-L. Li, X.-Y. Xu, G.-Y. Xiang, C.-F. Li, G.-C. Guo, *Realization of quantum Wheeler's delayed-choice experiment*, Nat. Photon. (2012).
13. R. Ionicioiu and D.R. Terno, *Proposal for a quantum delayed-choice experiment*, Phys. Rev. Lett. **107**, 230406 (2011).
14. M. Schirber, *Another Step Back for Wave-Particle Duality*, Physics **4**, 102 (2011).
15. A. Einstein, B. Podolsky, N. Rosen, *Can Quantum-Mechanical Description of Physical Reality Be Considered Complete?*, Phys. Rev. **47**, pp. 777-780 (1935).
16. J. S. Bell, *On the Einstein-Podolsky-Rosen Paradox*, Physics **1**, 195–200 (1964).
17. A. Aspect, J. Dalibard, G. Roger, *Experimental Test of Bell's Inequalities Using Time-Varying Analyzers*. Phys. Rev. Lett. **49**, pp. 1804–1807 (1982).
18. G. Weihs, T. Jennewein, C. Simon, H. Weinfurter, A. Zeilinger, *Violation of Bell's Inequality under Strict Einstein Locality Conditions*. Phys. Rev. Lett. **81**, pp. 5039–5043 (1998).
19. F. Kaiser, A. Issautier, O. Alibart, A. Martin, S. Tanzilli, *Guided-wave photonics for narrowband polarization entanglement*, e-print arXiv:1111.5683v1 (2011).
20. T. J. Herzog, P. G. Kwiat, H. Weinfurter, and A. Zeilinger, *Complementarity and the quantum eraser*, Phys. Rev. Lett. **75**, p. 3034 (1995).

21. J. F. Clauser, M. A. Horne, A. Shimony and R. A. Holt, *Proposed experiment to test local hidden-variable theories*, Phys. Rev. Lett. **23**, pp. 880-884 (1969).

22. S. S. Roy, A Shukla, T. S. Mahesh, *NMR implementation of a quantum delayed-choice experiment*, Phys. Rev. A **85**, 022109 (2012).

23. R. Auccaise, R. M. Serra, J. G. Filgueiras, R. S. Sarthour, I. S. Oliveira, L. C. Cĺeri, *Experimental analysis of the quantum complementarity principle*, Phys. Rev. A **85**, 032121 (2012).

24. J. F. Clauser, M. A. Horne, *Experimental consequences of objective local theories*, Phys. Rev. D **10**, p. 526 (1974).

25. A. Peruzzo, P. J. Shadbolt, N. Brunner, S. Popescu, J. L. O'Brien, *A quantum delayed choice experiment*, e-print arXiv:1205.4926v1 (2012).

26. X.-S. Ma, S. Zotter, J. Kofler, R. Ursin, T. Jennewein, C. Brukner, and A. Zeilinger, *Experimental delayed-choice entanglement swapping*, Nat. Phys. **8**, pp. 480-485 (2012).

We thank L. A. Ngah for his help on data acquisition and O. Alibart for fruitful discussions. Supported by the CNRS, l'Université de Nice - Sophia Antipolis, l'Agence Nationale de la Recherche for the 'e-QUANET' project (grant ANR-09-BLAN-0333-01), the European ICT-2009.8.0 FET open program for the 'QUANTIP' project (grant 244026), le Ministère de l'Enseignement Supérieur et de la Recherche (MESR), la Fondation iXCore pour la Recherche, and le Conseil Régional PACA for the 'QUANET' project.

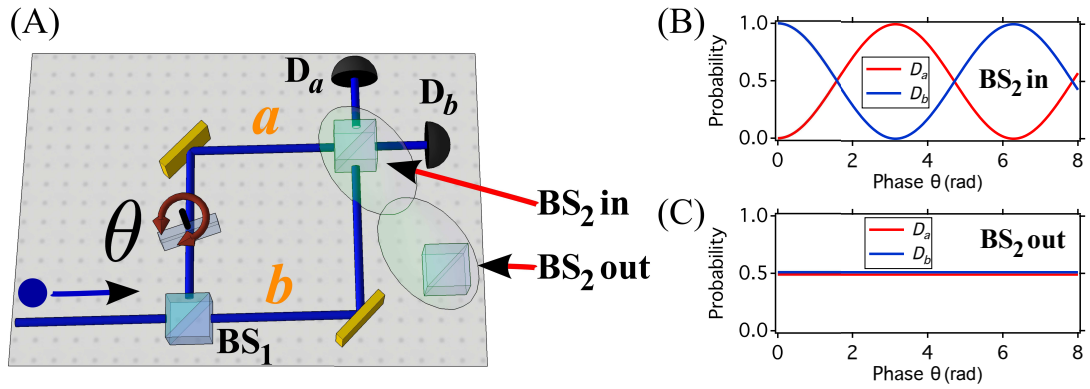

Fig. 1: (A) - Wheeler's gedanken experiment using a Mach-Zehnder interferometer. The device consists of two beam-splitters, BS_1 and BS_2, a glass plate introducing a phase shift θ, and two detectors, D_a and D_b, at its output. (B) - Simulated photon detection probabilities at detectors D_a and D_b as a function of the phase θ. The sinusoidal oscillations are related to unknown path information, and therefore to single photon interference, which is a wave-like phenomenon. (C) - Detection probabilities without BS_2. No interference is observed, which is the signature of particle behavior.

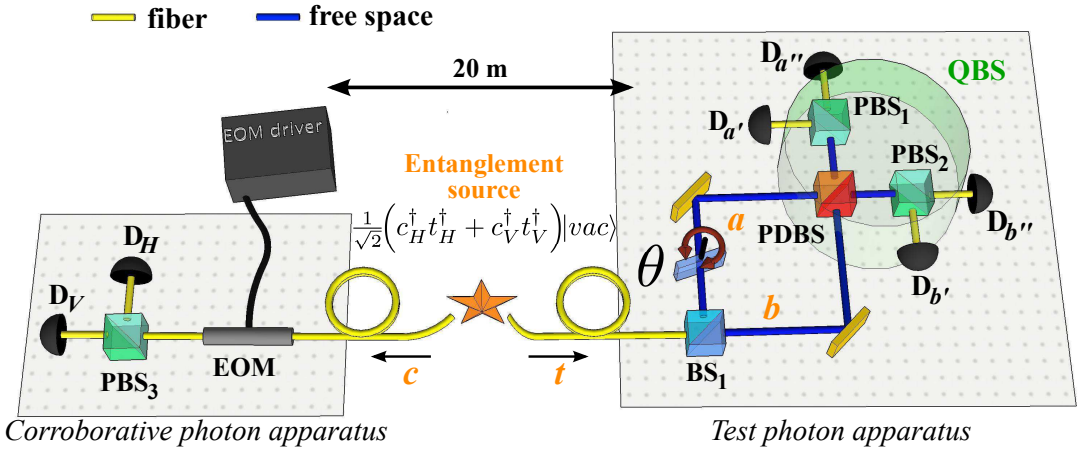

Fig. 2: Experimental setup. A source of polarization entangled photons ($\lambda = 1560$ nm, see (13)

for more details) sends, through a single mode optical fiber, one photon (t) to a quantum beam-splitter (QBS) apparatus, being an open (closed) Mach-Zehnder interferometer for horizontally (vertically) polarized photons. This is enabled by the use of a polarization dependent beam-splitter (PDBS). The second photon (c) of the entangled state is sent to another laboratory 20 m away (space-like separation), and used as a 'corroborative' photon which allows determining whether wave-like, particle-like, or both behaviors of photon t were observed.

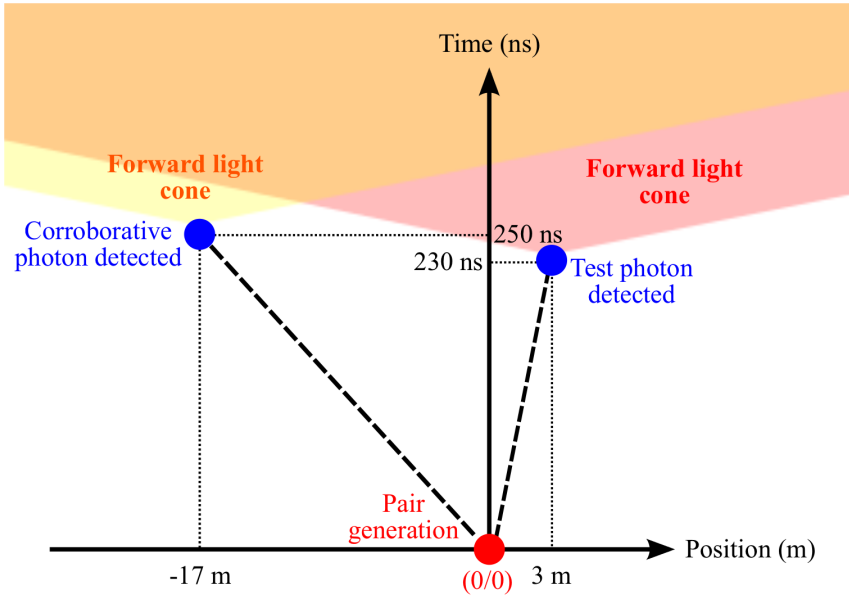

Fig. 3: Space-time diagram of the experimental apparatus. The paired photons are said to be generated and separated at the origin (0/0). The test photon travels about 50 m in an optical fiber before entering the QBS apparatus, that is located in the same laboratory as the entangled photon pair source. The corroborative photon is sent through a 55 m fiber to another laboratory. The corroborative and test photon apparatus are physically separated by 20 m. Note that the corroborative photon is measured 20 ns after the test photon was detected, thus revealing the Mach-Zehnder interferometer configuration in a delayed fashion. The forward light cones from both photon detection events do not overlap, demonstrating that space-like separation is

achieved. In other words, no causal connection between these events can be established.

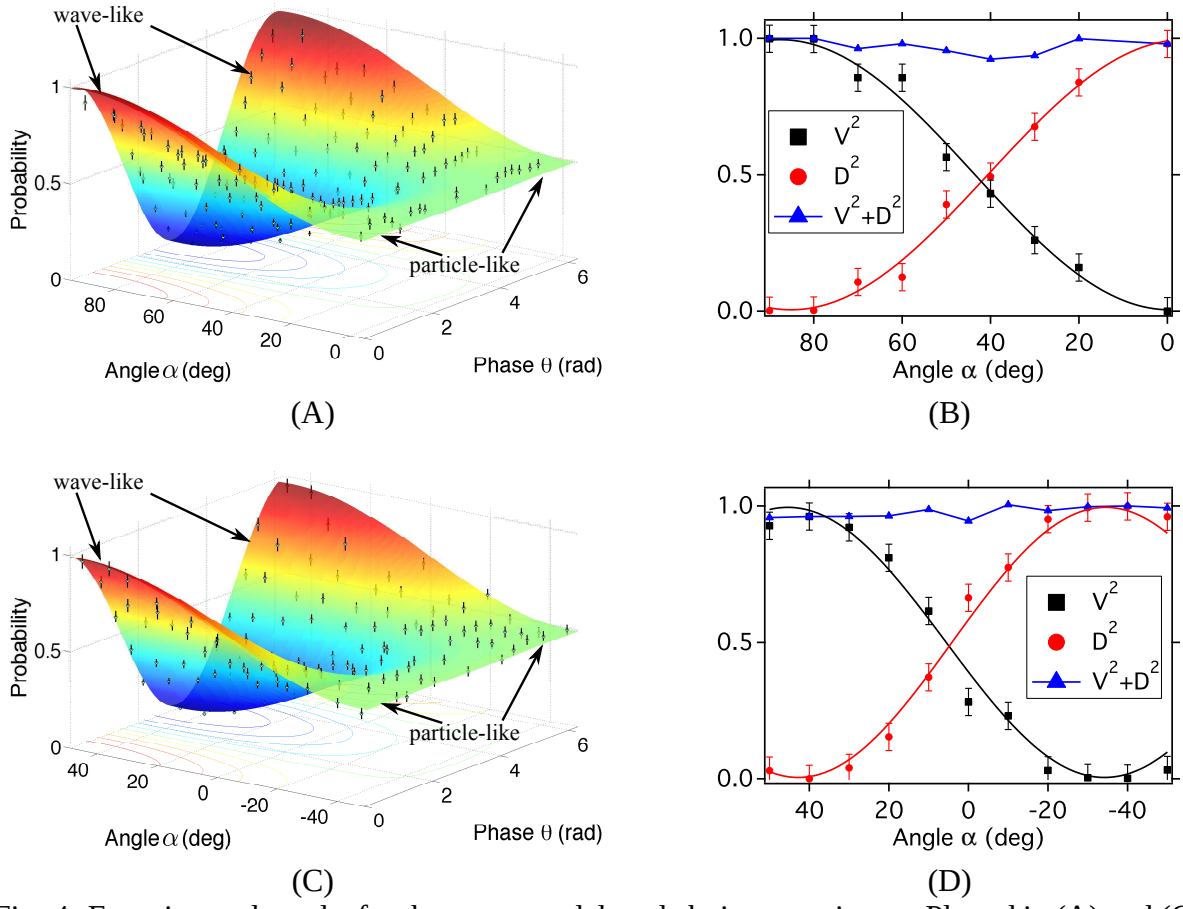

Fig. 4: Experimental results for the quantum delayed choice experiment. Plotted in (A) and (C) are the intensity correlations, $I_{H,b}(\theta, \alpha)$ as defined by Eq. 4, expressed as the probability of a coincidence event between detectors D_H and $(\mathrm{D}_{b'} \oplus \mathrm{D}_{b''})$ as a function of α and θ. Dots and associated vertical lines represent experimental data points and their corresponding standard deviations. Wave-particle morphing is observed for the natural $\{H, V\}$ basis (A), as well as for the complementary $\{D, A\}$ basis (C). The colored surfaces in these graphs represent the best fits to the experimental data using Eq. 4. Note that the result obtained for the $\{D, A\}$ basis is essential since it represents the signature of the entangled state, proving the correct implementation of the desired quantum beam-splitting effect. We obtain average coincidence rates

of 350 events/5 s. The noise contribution, on the order of 3 events/5 s, has not been subtracted. Figures (B) and (D) represent plots and related sinusoidal fits (solid lines) of the fringe visibility V (black) and path distinguishability D (red) as a function of the angle α. For all angles, we verify $V^2 + D^2 \leq 1$ as predicted by Eq. 5, the blue solid line being a guide for the eyes. Note that the same experimental results would be obtained if the timing order of the measurements of the test and corroborative photons would be inverted (*26*).

Supplementary information

S1: Experimental implementation of the PDBS

Note that the above introduced polarization dependent beam-splitter (PDBS) has been mimicked using a set of standard bulk optical components toward achieving high quality experimental results. The schematic is shown in Fig. S1.

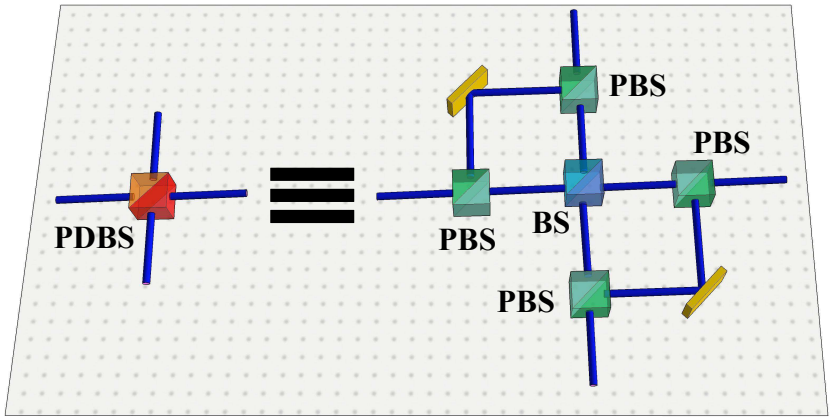

Fig. S1: In this realization the polarization dependent beam-splitters (PDBS), yielding the desired 100/0 reflection/transmission ratio for $|H\rangle$ and 50/50 reflection/transmission ratio for $|V\rangle$ was built using the bulk configuration shown. We used four polarizing beam-splitters (PBS) oriented in the $\{H, V\}$ basis. While $|H\rangle$ photons are reflected on each PBS and bypass the beam-splitter (BS), $|V\rangle$ photons are transmitted to an ordinary 50/50 BS. Commercially available PDBS devices show seriously reduced performance and would have significantly reduced the measured visibilities.

S2: Measurement of fringe visibility and path distinguishability

The interference fringe visibility V shown in Fig. 4(B,D) is measured as follows. The angle α is fixed and the maximum ($p_{\max}$) and minimum ($p_{\min}$) fitted coincidence probabilities are determined as a function of θ. We then compute $V = (p_{\max} - p_{\min})/(p_{\max} + p_{\min})$.

D is measured for fixed angles α using the following procedure. First, the interferometer path a is blocked and the coincidence probabilities p_{aa} between detectors D_H and ($\mathrm{D}_{a'} \oplus \mathrm{D}_{a''}$) and p_{ab} between detectors D_H and ($\mathrm{D}_{b'} \oplus \mathrm{D}_{b''}$) are recorded. Here, the first subscript denotes the blocked interferometer arm and the second which detector combination is used. We then compute $D_a = (|p_{aa} - p_{ab}|)/(p_{aa} + p_{ab})$. Note that complete path distinguishability leads to $p_{aa} = 0$ and $p_{ab} = 1$, resulting in $D_a = 1$. The same measurement is repeated when interferometer path b is blocked, giving the probabilities p_{ba}, p_{bb}, and consequently $D_b = (|p_{ba} - p_{bb}|)/(p_{ba} + p_{bb})$. We finally calculate the average $D = (D_a + D_b)/2$, which drops to zero for wave-like behavior and is unity for particle-like behavior.